Calcif Tissue Int (1998) 63:475–481

Calcified Tissue International
© 1998 Springer-Verlag New York Inc.

Laboratory Investigations

MicroRaman Spectral Study of the PO_4 and CO_3 Vibrational Modes in Synthetic and Biological Apatites

G. Penel,[1] G. Leroy,[1] C. Rey,[2] E. Bres[3]

[1]L.B.M.-Microspectrométrie Raman faculté d'Odontologie, Place de Verdun 59045 Lille, France
[2]Laboratoire des Matériaux-Physico-Chimie des Solides, Ecole Nationale Supérieure de Chimie, UPRESA 5071, 38, rue des 36 Ponts, 31400 Toulouse, France
[3]Laboratoire de Structure et des Propriétés de l'Etat Solide, LSPES URA CNRS 234, USTL Bât. C6 59655 Villeneuve d'Ascq, France

Received: 5 January 1998 / Accepted: 12 May 1998

Abstract. The carbonate and phosphate vibrational modes of different synthetic and biological carbonated apatites were investigated by Raman microspectroscopy, and compared with those of hydroxyapatite. The ν_1 phosphate band at 960 cm^{-1} shifts slightly due to carbonate substitution in both A and B sites. The spectrum of type A carbonated apatite exhibits two ν_1 PO_4^{3-} bands at 947 and 957 cm^{-1}. No significant change was observed in the ν_2 and ν_4 phosphate mode regions in any carbonated samples. The ν_3 PO_4^{3-} region seems to be more affected by carbonation: two main bands were observed, as in the hydroxyapatite spectrum, but at lower wave numbers. The phosphate spectra of all biominerals apatite were consistent with type AB carbonated apatite. In the enamel spectrum, bands were observed at 3513 and at 3573 cm^{-1} presumably due to two different hydroxyl environments. Two different bands due to the carbonate ν_1 mode were identified depending on the carbonate substitution site A or B, at 1107 and 1070 cm^{-1}, respectively. Our results, compared with the infrared data already reported, suggest that even low levels of carbonate substitution induce modifications of the hydroxyapatite spectrum. Increasing substitution ratios, however, do not bring about any further alteration. The spectra of dentine and bone showed a strong similarity at a micrometric level. This study demonstrates the existence of acidic phosphate, observable by Raman microspectrometry, in mature biominerals. The HPO_4^{2-} and CO_3^{2-} contents increase from enamel to dentine and bone, however, these two phenomena do not seem to be correlated.

Key words: Raman microspectrometry — Carbonated apatite — Enamel — Dentine — Bone.

Calcium phosphate of vertebrate hard tissue exhibits an apatitic structure. However, many variations in composition and structure within the same tissue have been reported. These variations are influenced by the animal's age, dietary history, and health status, hence the challenge to characterize these biominerals. Biological apatites are usually described as substituted hydroxyapatite [OHAp: Ca_{10} $(PO4)_6$ $(OH)_2$]. Most biominerals contain carbonate but its influence on biological crystal is not clear. This is why the study of these minerals is of interest in biomineral composition and structures understanding [1–8].

Two types of carbonate substitutions have been described in synthetic compounds: type A (OH^- substituted by CO_3^{2-}) and type B (PO_4^{3-} substituted by CO_3^{2-}). Previous Raman studies on carbonated apatites have reported variable numbers of bands in the ν_3 PO_4^{3-} domain. Despite these discrepancies, two main bands are consistently reported to be around 1070 and 1046 cm^{-1}. Two distinct wavenumbers of the ν_1 carbonate mode have been suggested depending on whether substitution is of type A or B [9–11] at 1108 and 1070 cm^{-1}, respectively.

Dental enamel is the most mineralized tissue of the human body (97 wt%). The carbonate content represents 2–4 wt% [12–14] with a reported 90% of type B and 10% of type A [14]. Mature bone mineral and dentine generally contain more carbonate (5–8 wt% of the mineral); the distribution between type A and B sites has not been determined precisely although it has been reasonably assumed that type B carbonate is the major species [15, 16]. The existence of HPO_4^{2-} and nonapatitic environments of phosphate and carbonate ions in calcium phosphate biominerals have also been established. Differences in the concentrations of HPO_4^{2-} and CO_3^{2-} groups have been observed in calcified cartilage and bone, and related to tissue formation and maturation [17–19].

One of the problems linked to the use of infrared (IR) and Raman (R) methods is the identification of bands, especially in complex, substituted, biological apatites. The vibrational activity is different in R and IR, some modes are both IR and R active, but others are only R or IR active. Both R and IR band positions are influenced by both composition and structure, especially symmetry changes (like the space group for crystals). Thus, synthetic samples, generally having a better crystallinity than biological apatites,

Correspondence to: G. Penel, L.B.M.-Microspectrométrie Raman faculté d'Odontologie, Place de Verdun 59045 Lille, France

are used as models to investigate complex biological compounds [20]. Several studies using FTIR microspectroscopy in mineralized tissues have been reported [21–24]. Such investigations are usually performed in the transmission mode and need specific sample preparation. Besides, the micro-Raman probe of the micrometric scale is 10–100 times smaller than the probe used for IR microspectrometry. Raman microspectrometry also permits investigations of samples without possible artifacts due to specimen preparation. This method, used in the reflection mode, is nondestructive, thus different regions, such as interfaces, of the sample can be investigated. The micrometric probe size reduces the fluorescence problems encountered in conventional Raman spectroscopy on such natural materials. The vibrational modes of PO_4^{3-}, OH^-, HPO_4^{2-}, and CO_3^{2-} groups can be studied by Raman spectroscopy. In addition, the relative intensities of bands between normalized spectra can lead to quantitative estimations of these constituents. Thus, Raman microspectrometry can give new and complementary information about biominerals with a micrometric probe.

There have been very few studies on Raman methods of carbonated apatites, dental enamel, dentine, and bone. For dental enamel, most studies have been done by conventional Raman methods [4, 17] on powdered samples. Because of the small amounts of carbonate ions in this tissue, the spectra are generally interpreted by reference to hydroxyapatites [9, 14.]. Conventional Raman spectroscopic investigations on bone are usually difficult because of fluorescence problems related to organic components [17, 25], and the deproteination treatments proposed to solve this problem [26] are drastic. They disrupt the three-dimensional organization of the tissue, and might alter minor constituents themselves or their environments.

The aim of this work was to study different synthetic and biological carbonated apatites with a Raman microspectrometric technique in order to specify band assignments and spectral alterations due to carbonate incorporation and crystallinity.

Materials and Methods

Preparation of Synthetic Samples

Type B carbonate apatite (BCarAp): a phosphate solution [$(NH_4)HPO_4$: 200 g; $NaHCO_3$: 42 or 21 g; ammonia solution (sp. gravity: 0.93): 500 ml; H_2O: 3000 ml], was added slowly (for 3 hours) to a stirred calcium solution [$Ca(NO_3)_2$. $4H_2O$: 472 g; ammonia solution (sp. gravity: 0.93): 1000 ml; H_2O : 3000 ml] at 80°C. The precipitate was left to mature for 1 hour before filtration. It was then washed with distilled water and dried at 80°C. Two samples corresponding to a carbonate-rich and to a carbonate-poor apatite were prepared.

Type A carbonate apatite (ACarAp) was prepared from a stoichiometric hydroxyapatite (OHAp), synthesized by Trombe's method [9], by treatment in a dry CO_2 atmosphere for 3 days at a high temperature (900°C).

The HPO_4-containing apatite was prepared by hydrolysis of β tricalcium phosphate (TCP) in boiling water [27].

Purity of samples was monitored by chemical analysis, X-ray diffraction, and FTIR spectroscopy. No sample was found to contain impurities. The carbonate content of ACarAp was 5.8 wt% and OH^- groups were not observed by either R or IR spectroscopy. The three samples of BCarAp contained, respectively, 4.5, 7, and 10 wt% carbonate.

Powders were spread on a microscope slide for spectral acquisition.

Preparation of Biological Samples

For dental samples, sound first premolars extracted for orthodontic reasons from 12-year-old children were used. The root was cut off with a high-speed dental burr under water spray. The crown was fractured along the longitudinal axis with a surgical instrument placed between cusps. Then the dental samples were oriented on the microscope slides in transverse excitation/detection arrangements, as described by Tsuda and Arends [28].

Bone samples were obtained from rabbit femur cleaned and broken in the middle of the diaphysis. To eliminate fluorescence artifacts, the samples were immersed successively for 2 hours at room temperature in acetone, then in a 30% hydrogen peroxide solution, and in acetone again. The samples were dried at room temperature and placed on a microscope slide for spectral acquisition [29]. All assays were performed on about 30 biological samples.

Raman Microspectrometry

We used a OMARS89 microspectrometer from DILOR (Lille, France) with helium neon (632 nm) laser excitation at a power of 3 mW reaching the sample. The overall spectral resolution was 2 cm^{-1}. The spectra were obtained in the 200–3700 cm^{-1} range. The ×100 microscope objective used in a confocal configuration give a micrometric spot size. For easier comparison, all spectra are presented with a normalized intensity. This normalization was obtained by computation of spectra with equal intensity value of the ν_1 PO_4^{3-} band.

Results

Raman band positons and assignments are listed in Table 1 and compared with those of hydroxyapatite [30].

Phosphate Vibrational Modes

The ν_1 mode of phosphate at 964 cm^{-1} for hydroxyapatite exhibited a slight wave number shift in type B carbonated apatites. We observed a single band at 960 cm^{-1}, a position that did not seem to change with the rate of carbonate substitution. The ACarAp, on the contrary, exhibited two bands, the most intense at 957 cm^{-1}, and a distinct shoulder at 947 cm^{-1} (Fig. 1). In biological samples the ν_1 mode of phosphate exhibited the same modifications as synthetic type B samples: a single band around 960 cm^{-1} was observed [31]. In enamel, this single band seems stronger than the one observed in dentine and bone spectra.

The ν_2 domain of synthetic samples was seen to be different depending on the type of substitution. In ACarAp, a broad band with several poorly resolved shoulders was observed at 440 cm^{-1}. For BCarAp and enamel spectra, the ν_2 PO_4^{3-} mode wave number positions were nearly the same with two bands around 432 and 445 cm^{-1}. In dentine and bone samples, the band at 432 cm^{-1} was conserved but the second shifted slightly to 450 and 452 cm^{-1}, respectively (Fig. 2).

The ν_3 PO_4^{3-} domain appears to be the most affected by carbonate substitution. As already reported in a previous study on fluoride-substituted OHAp [30] the number of bands decreased and the region was dominated by two main bands with a significant shift compared with OHAp (see Table 1). These main bands dominate this spectral region on synthetic type B, and on biological apatite samples at similar wave number values of around 1046 and 1070 cm^{-1}. However, the 1070 cm^{-1} band cannot be assigned to phosphate ions alone as it corresponds also to the ν_1 mode of carbonate ions. The intensity of this band increased with

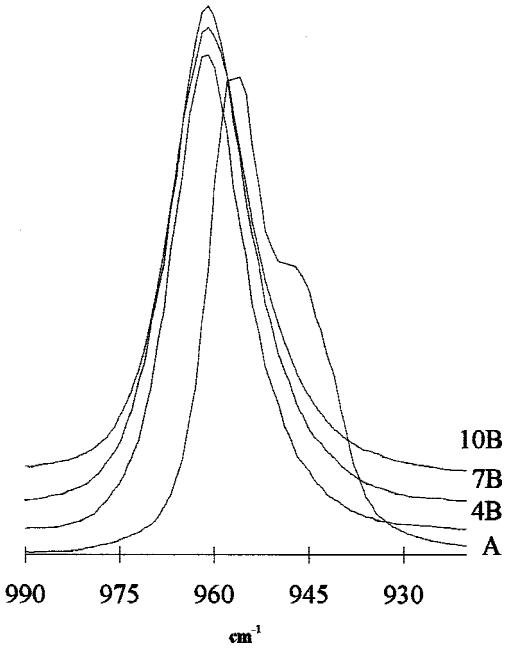

Fig. 1. Raman spectra in the ν_1 phosphate mode region of (A) 5.8 wt% type A carbonated apatite, (4B) 4.5 wt% type B carbonated apatite (7B), 7 wt% type B carbonated apatite (10B) 10 wt% type B carbonated apatite.

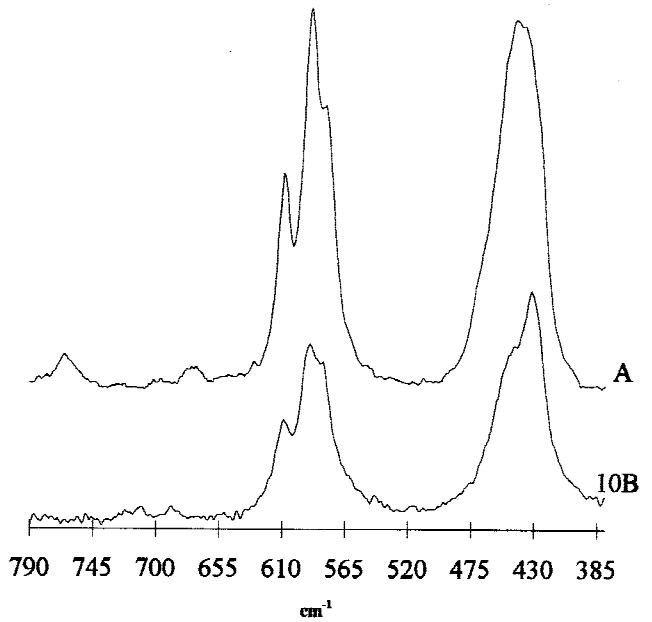

Fig. 2. Raman spectra in the ν_2 and ν_4 modes of phosphate, and the ν_4 mode of carbonate region of (A) 5.8 wt% type A carbonated apatite, (10B) 10 wt% type B carbonated apatite.

type B carbonate content. In AcarAp spectra, three bands were detected at 1018, 1031, and 1059 cm^{-1}. This feature was not observed on any other type B carbonate-containing apatites, and seems characteristic of ACarAp (Fig. 3). The two main bands at 1031 and 1059 cm^{-1} can be considered as shifted bands observed in the other CarAp. The shift could be due to strong environmental modifications of PO_4^{3-} ions induced by complete hydroxyl substitution. In spectra of biological samples, the frequency shift was negligible, and a regular type A environment in these samples represents a minor proportion of the carbonate substitution.

The PO_4^{3-} ν_4 mode always exhibited three main bands with constant wave number values (579, 590, and 608 cm^{-1}). The band around 590 cm^{-1} exhibited the strongest intensity in all the synthetic and biological samples. In comparison with the OHAp spectra, the weak band at 614 cm^{-1} was not observed in all carbonated samples, presumably due to band broadening. In the ACarAp spectrum, a band was detected at 630 cm^{-1}. In OHAp, the 630 cm^{-1} band assigned to the OH^- libration mode has been sometimes reported, and was not observed by us. In ACarAp this band cannot be due to the hydroxyl groups undetected in this sample by IR. It cannot be definitely attributed to PO_4^{3-} groups, however, as it was observed at a wave number significantly higher than that of the other ν_4 PO_4^{3-} bands. So, its assignment remains uncertain (Fig. 2).

On the HPO_4^{2-}-containing apatites, two additional bands attributed to acidic phosphate ions were observed at 1003 and 873 cm^{-1} (Fig. 6).

Hydroxyl Modes

The enamel spectrum exhibited two bands: one at 3573 (common with OHAp) and to our knowledge, an unreported one at 3513 cm^{-1} (Fig. 4). Observation of this band was impossible in dentine and bone spectra because of the broad water band (3513 cm^{-1}) (Fig. 5). In addition, to our knowledge, these ions have never been detected by IR in bone and dentine. The second band (3513 cm^{-1}) observed in the OH^- stretching mode region was not detected in synthetic carbonated samples and cannot be assigned to carbonation. It could be due to a OH^- ion interacting by hydrogen bonding with another anion. The shifts due to F-OH or Cl-OH interactions are stronger in stoichiometric apatites [14], however, the evolution of this type of interaction in carbonated samples is unknown.

Carbonate Modes

Types A and B ν_1 carbonate bands were detected separately, at 1103 and 1071 cm^{-1}, respectively. These bands were identified in all synthetic and biological samples. Although type B carbonate band superimposes on the ν_3 phosphate band, the frequency shift from 1077 to 1071 cm^{-1} in OHAp indicates a type B carbonation. The intensity of the 1071 cm^{-1} band increased consistently with the carbonate content in both synthetic and biological samples and most of its intensity was due to carbonate ions in apatites containing more than 4% type B carbonate. The type A ν_1 carbonate band shifted slightly, in all biological samples, to 1103 cm^{-1} but remained observable. This band was very weak for enamel and increased in bone and dentine consistently with the total carbonate content. The two bands due to the ν_4 carbonate mode were identified, in the ACarAp, at the same wave number as in infrared spectra [18, 19] 675 and 765 cm^{-1} (Fig. 3). In spectra of 10% BCarAp, a very weak band appeared at 751 cm^{-1}, whereas in other BCarAp, two very weak bands were detected at 716 and 690 cm^{-1} [4].

The ν_3 carbonate domain could not be investigated because of the weakness of the bands and their superimposi-

Table 1. Raman band positions and assignments compared with those of hydroxyapatite

	OHAp	ACarAp	BCarAp 4.5%	BCarAp 7%	BCarAp 10%	Enamel	Dentine	Bone
$v_2PO_4^{3-}$	433		432	432	432	433	432	432
		440						
	448		445	445	445	450	450	452
$v_4PO_4^{3-}$	580	579	579	579	579	579	580	584
	591	589	590	590	590	588	590	590
	607	608	609	609	609	608	610	611
	614							
NA		630						
$v_4\ CO_3^{2-}$		675						
		765						
P-OH stretch							873	873
?							920	924
$v_1\ PO_4^{3-}$	964	947	961	961	961	959	959	961
		957						
$v_1\ HPO_4^{2-}$						1002	1003	1005
$v_3\ PO_4^{3-}$	1029	1018	1030	1030	1026	1026	1031	1032
	1034							
	1041							
	1048	1031	1045	1046	1047	1043	1046	1044
	1057							
	1064							
	1077	1059	1070	1071	1070	1071	1069	1071
B type $v_1\ CO_3^{2-}$					1070	1071	1069	1071
A type $v_1\ CO_3^{2-}$		1107				1103	1102	1103
Amide III							1245	1243
[27, 37]							1260	1262
C-H bending							1450	1449
[21, 37]								
Amide I							1660	1662
[21, 37]								
C-H							2881	2882
stretching							2948	2946
[21, 37]							2923	
							2988	2986
OH stretch						3513		
	3573				3576	3573	NO	NO

NO = not observed; NA = not assigned

tion on organic matter bands in biological samples. The ν_2 domain did not show any identifiable bands.

Discussion

Several studies have been reported on carbonated apatites [5, 9, 10, 18, 19]. A first question is related to the effect of carbonate uptake on Raman spectra, especially on the number of bands and their wavenumber assignment. This point is crucial for further, more detailed studies of spectra and band identification of nonapatitic environments, for example, which have been found in the initial deposits of calcified tissues.

The substitution of carbonate ions for OH^- or PO_4^{3-} ions induces the creation of vacancies and distortions in the atomic arrangement.

For type A carbonate apatite the substitution of a monovalent ion by a divalent one is compensated for by the creation of a vacancy and the chemical composition can be represented by:

$$Ca_{10}(PO_4)_6CO_3\square$$

where $\square$ represents the vacancy.

This substitution results in the loss of the 6_3 screw axis but preserves the existence of the C_3 axis. Thus, the six phosphate groups of the unit cell are no longer equivalent in the lattice but may be split into two groups, one organized around a vacancy and one around a carbonate ion, as suggested by Trombe [7]. The shoulder and main band observed in the ν_1 mode region of phosphate in ACarAp can be assigned to two different environments (vacant sites or divalent ions) of the phosphate groups in planes ¼ and ¾ [7, 8, 32]. It should be noted, however, that vibrational correlations could occur between equivalent phosphates and that theoretically two ν_1 bands should be seen in this domain for each group of three phosphate ions. Similar observations were made on oxyhydroxyapatites $(Ca_{10}(PO_4)_6(OH)_{2-2x}O_x\square_x$; $0 \leqslant \times \leqslant 1$ and where $\square$ is a OH^- ion vacancy), where the ionic distribution along the *c* axis is also disturbed, but in this case, other vibrational domains are also strongly altered. The existence of two different types of phosphate environments in oxyapatite has recently been confirmed by MAS-NMR [33]. Such a modification of the environment should affect the other phosphate modes as it does in IR [8]. Raman spectra modifications in the ν_3 and ν_4 domains are, however, more difficult to assess and it is actually impossible to distinguish the two

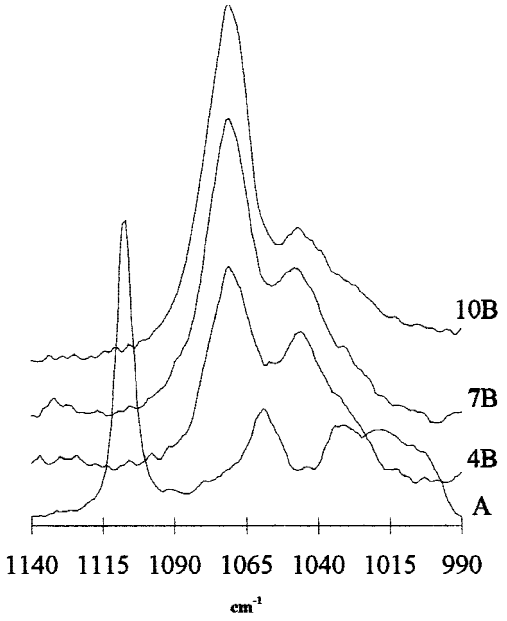

Fig. 3. Raman spectra in the ν_3 phosphate mode region of (A) 5.8 wt% type A carbonated apatite, (4B) 4.5 wt% type B carbonated apatite, (7B) 7 wt% type B carbonated apatite, (10B) 10 wt% type B carbonated apatite.

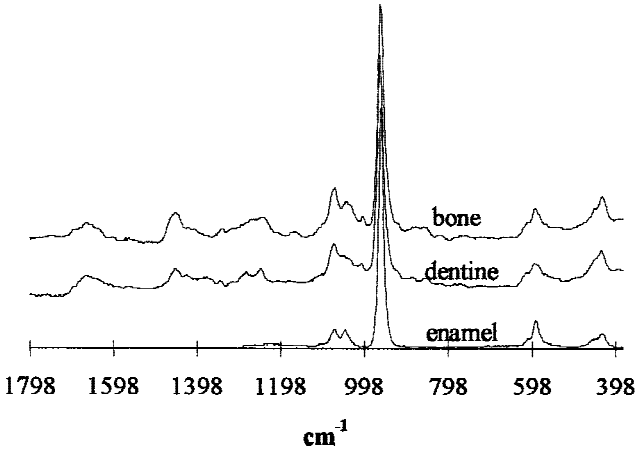

Fig. 4. Raman spectra of human enamel and dentine, and rabbit bone in the 1800-380 cm^{-1} region.

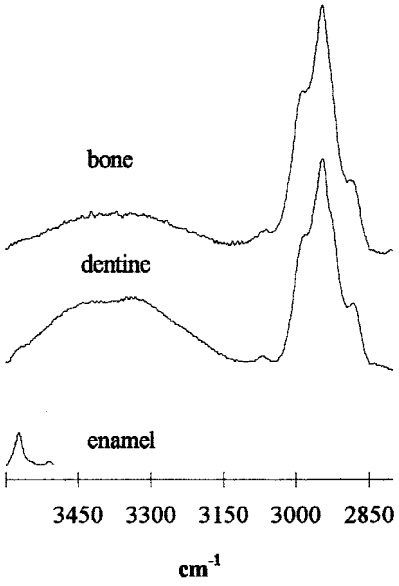

Fig. 5. Raman spectra of human enamel and dentine, and rabbit bone in the 3600-2800 cm^{-1} region.

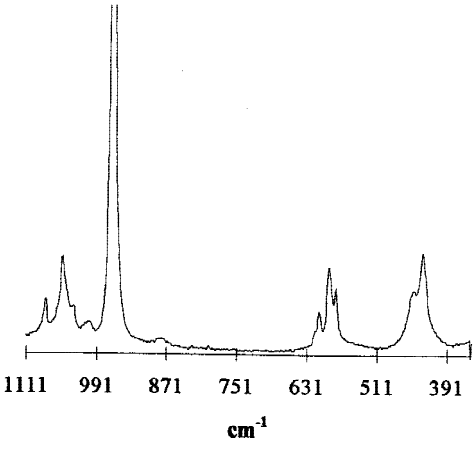

Fig. 6. Raman spectra of well-crystallized HPO_4^{-2} containing apatite in the 350-1111 cm^{-1} region.

phosphate groups like for ν_1. Previous Raman studies on synthetic apatites containing 2.2–12.4 wt% AB type carbonate prepared from solutions at 80°C, have shown two bands in the ν_3 PO_4^{3-} domain (at 1069-1072 and 1044-1046 cm^{-1}) [4]. For carbonated apatites prepared from solutions at 42°C, three bands have been observed (at 1031, 1048, 1076 cm^{-1}) [5]. Synthetic, well-crystallized AB-type carbonated apatites obtained at 900–950°C, showed either four bands (at 1029, 1042, 1047, 1075 cm^{-1}) [6] or three bands (at 1029, 1048, 1075 cm^{-1}) [9] with variable carbonation levels (7.88 and 11.8 wt%, respectively). In the present study, the band broadening and disymmetry compared with well crystallized OHAp suggest, however, some overlapping. The 1018 cm^{-1} band, also observed in oxyhydroxyapatites, could be characteristic of apatites containing divalent ions and vacancies instead of monovalent ions. However, the ν_2 and ν_4 domains did not show any specific bands associated with carbonation.

The type A ν_1 carbonate band at 1107 cm^{-1} is very specific of carbonate groups substituting OH^- ions and can be considered as a signature. This band appears clearly in enamel. In dentine and bone it appears as weaker but broader but nevertheless, clearly apparent. This observation confirms the existence of type A carbonate in bone and dentine as suggested by IR data [16]. The relative intensity of the 1103 cm^{-1} band indicates that the proportion of type A carbonate is similar in enamel, dentine, and bone.

For type B carbonate the substitution of a PO_4^{3-} group by a CO_3^{2-} mainly causes the creation of a Ca^{2+} vacancy and a OH^- vacancy. These compounds can be represented by:

$$Ca_{10-x+u}\,\square_{x-u}\,(PO_4)_{6-x}\,(CO_3)_x\,OH_{2-x+2u}\square_{x-2u}$$

with $0 < x < 2$ and $0 < u < x$. For our compounds the values of u and x can be determined from the chemical composition.

These substitutions have several consequences on the crystal lattice and in the Raman spectra. If we assume a statistical distribution of the carbonate and phosphate groups, the periodicity of the lattice is altered and factor group considerations, especially, are no longer valid for the high to medium substitution range. Site symmetry alone should be adequate for interpretation of the spectroscopic data. The substitution of one PO_4^{3-} in the unit cell by a CO_3^{2-} for example, which is the case for apatites containing around 6% carbonate, destroys the main symmetry elements and all phosphate groups become independent which does not allow correlations between vibrational movements. In addition, the local environments of the groups can be modified by vacancies and/or substituents leading to different vibrational frequencies and/or band broadening. In the case of bone and dentine mineral, the small size of the crystals adds its effect to carbonate substitution for phosphate. Despite the low crystallinity, the band broadening with respect to well-crystallized carbonated apatites is minor. For these samples, the lack of periodicity and symmetry elements, if we assume a statistic distribution of the substituents and defects, should give spectra that are interpretable from the point of view of site symmetry only.

The phosphate bands observed in substituted type B carbonate-containing apatites spectra are broader and less intense than those of OHAp. The observation of a strong single ν_1 band, two bands in the ν_2 domain, and three main bands in the ν_3 and ν_4 domains at identical wave-number values indicates, however, that differences in the environment of the phosphate groups in type B carbonate-containing apatites are negligible in the concentration range used in this study. Type B carbonate should disrupt the symmetry between the PO_4^{3-} groups in planes at ¼ *c* and ¾ *c*, thus, common R and IR bands should be observed [30]. But, the detected Raman bands differ from IR band positions (Table 1). This observation is not consistent with site symmetry considerations only and could indicate that some local organization exists, allowing correlations of vibrational movements. In particular, the most intense IR band at 560 cm^{-1} is not observed on the Raman spectra. Conversely, the most intense Raman bands at 590 and 579 cm^{-1} are not observed on the IR spectra [18].

The spectra of type B carbonated apatites are analogous to those of enamel which is not surprising considering the site A low occupancy. The type A ν_1 carbonate band, at 1106 cm^{-1}, is only apparent in the spectra as a very weak band and the ν_1 PO_4^{3-} mode does not show the characteristics of type A carbonated samples. For these samples with a low carbonate content, the distinction between two types of carbonate substitution seems easier on IR than on Raman spectra. But it should be emphasized that a small amount of carbonate substituting phosphate ions is enough to modify the Raman spectra of OHAp in the ν_3 domain of PO_4^{3-}, as reported with FTIR [19]. The superimposition of the most intense carbonate band on a phosphate band complicates the analysis. However, it can be noticed that the ν_1 PO_4^{3-} band appears in a domain where no other intense band due to organic matter or carbonate exist. Therefore, this band can be used as a reference to normalize the spectra. The relative intensity of the 1070 cm^{-1} band can give a good estimation of the type B carbonate content. All biological samples conform to type B apatite spectra with slight shifts and changes in intensities. Previous studies of synthetic high-temperature carbonate apatites [9] and apatites produced from aqueous solutions at 42°C [5] have reported a relationship between the ν_1 of PO_4^{3-} band half-width and the carbonate content. In the present study, these modifications between type B 4.5%, 7% and 10 wt% apatites are significant (13, 15, and 17 cm^{-1}, respectively). Dentine and bone have similar values, (20 and 18 cm^{-1}, respectively) but enamel exhibits a lower value (14 cm^{-1}) consistent with its lower carbonate content and higher crystallinity.

Another interesting question is related to the detection of nonapatitic environments by Raman spectroscopy as they have been detected by IR. A faint band is observed around 1003 cm^{-1} with an insignificant wave number shift in all biological samples. This band was also observed in Raman spectra of well-crystallized apatites that contained HPO_4^{2-} ions. It does not appear in synthetic type B carbonated apatites obtained in alkaline conditions. In agreement with other authors, this band can be assigned to HPO_4^{2-} groups, it is observed in nonapatitic Ca-P like octacalcium phosphate (OCP) [34], and has also been reported in biological mineral [17]. Other faint bands around 920–924 cm^{-1} can also be noted in dentine and bone, but not in synthetic HPO_4^{2-}-containing apatites. These bands have also been reported by others [17, 35] and assigned to HPO_4^{2-} groups in an OCP environment. However, similar bands observed by IR in calcifying cartilage have been shown to be due to organic components [36], thus, the origin of these bands is not yet certain. The detection of these species seems to be more difficult with Raman than with IR. Most phosphate vibrational domains show weak bands that cannot be easily decomposed or deconvoluted. The most sensitive Raman band (in the ν_1 domain) shows alterations, especially band broadening, mainly associated with carbonation, that have been observed by several authors. The possible existence of an additional broad phosphate band around 920 cm^{-1}, possibly corresponding to nonapatitic species, has to be confirmed. The bands around 873 cm^{-1} have been reported by IR studies on biological apatite crystals, and assigned to carbonate [36] and HPO_4^{-2} ions [25]. In the present study, a band in this domain observed in synthetic HPO_4^{2-}-containing apatite was absent from all synthetic carbonated samples, and thus it can be reasonably assigned to HPO_4^{2-} in biological samples.

References

1. Brès EF, Barry JC, Hutchison JL (1985) High-resolution electron microscope and computed images of human tooth enamel crystals. J Ultrastruct Res 90:261–274
2. Voegel JC, Frank RM (1977) Ultrastructural study of apatite crystal dissolution in human dentine and bone. J Biol Buccale 5:181–194
3. Goldberg M (1989) Manuel d'histologie et de biologie buccale. Editor Masson, Paris
4. Nishino M, Yamashita S, Aoba T, Okazaki M, Moriwaki Y (1981) The laser-Raman spectroscopic studies on human enamel and precipitated carbonate-containing apatites. J Dent Res, 60(3):751–755
5. De Mul FFM, Hottenhuis MHJ, Bouter P, Greve J, Arends J, Ten Bosch JJ (1986) Micro-Raman line broadening in synthetic carbonated hydroxyapatite. J Dent Res 65:437–440
6. Nelson DGA, Featherstone JDB (1982) Preparation, analysis, and characterisation of carbonated apatites. Calcif Tissue Int 34:69–81
7. Trombe JC (1973) Contribution à l'étude de la décomposition et de la réactivité de certaines apatites hydroxylées et carbonatées. Ann Chim Paris 8:251–269
8. Trombe JC, Montel G (1973) Sur le spectre d'absorption in-

frarouge des apatites dont les tunnels contiennent des ions bivalents et des lacunes. C R Acad Sci Paris Ser C, 276:1271–1274
9. Nelson DGA, Williamson BE (1982) Low-temperature laser Raman spectroscopy of synthetic carbonated apatites and dental enamel. Aust J Chem 35:715–727
10. Trombe JC (1972) Contribution à l'étude de la décomposition et de la réactivité de certaines apatites hydroxylées, carbonatées ou fluorées alcalino-terreuses. Thèse Université de Toulouse
11. Fowler BO (1977) I. Polarised Raman spectra of apatites II. Raman bands of carbonate ions in human tooth enamel. Miner Tissue Comm 3:68
12. Legeros RZ (1990) Chemical and crystallographic events in the caries process. J Dent Res 69(spec. issue):567–574
13. Apap M, Goldberg M (1985) A new microsample grinding technique for quantitative determination of calcium and phosphorus in dental enamel. J Dent Res 11:1293–1295
14. Elliott JC (1994) Structure and chemistry of the apatites and other calcium orthophosphates. Studies in inorganic chemistry. Elsevier, Amsterdam, London, New York, Tokyo, pp 63 and 230
15. Legeros RZ (1994) Biological and synthetic apatites. In: Brown P, Constantz B (eds) Hydroxyapatites and related compounds. CRC Press, Boca Raton, pp 3–28
16. Rey C, Collins B, Goehl T, Dickson RI, Glimcher MJ (1989) The carbonate environment in bone mineral. A resolution enhanced Fourier transform infrared spectroscopy study. Calcif Tissue Int 45:157–164
17. Sauer GR, Zunic WB, Durig JR, Wuthier RE (1994) Fourier Transform Raman spectroscopy of synthetic and biological calcium phosphates. Calcif Tissue Int 54:414–420
18. Rey C, Shimizu M, Collins B, Glimcher MJ (1990) Resolution-enhanced Fourier Transform infrared spectroscopy study of the environment of phosphate ion in the early deposits of a solid phase of calcium phosphate in bone and enamel and their evolution with age: I. Investigation of the ν_4 PO_4^{3-} domain. Calcif Tissue Int 46:384–394
19. Rey C, Shimizu M, Collins B, Glimcher MJ (1991) Resolution-enhanced Fourier Transform infrared spectroscopy study of the environment of phosphate ion in the early deposits of a solid phase of calcium phosphate in bone and enamel and their evolution with age: II. Investigations in the ν_3 PO_4^{3-} domain. Calcif Tissue Int 49:383–388
20. Barroug A, Rey C, Trombe JC (1994) Precipitation and formation of type AB carbonate apatite analogous to dental enamel. In: Advanced materials research, physical chemistry of solid-state materials, REMCES VI. Aride J et al. (eds), pp 147–153
21. Nie S, Bergbauer KL, Ho JJ, Kuck J, Yu N (1990) Application of near-infrared Fourier transform Raman spectroscopy in biology and medicine. Spectroscopy Int 3(1):20–26
22. Gadaleta SJ, Landis WJ, Boskey AL, Mendelsohn R (1996) Polarized FT-IR microscopy of calcified turkey leg tendon. Connect Tissue Res 34:203–211
23. Gadaleta SJ, Camacho NP, Mendelsohn R, Boskey AL (1996) Fourier transform infrared microscopy of calcified turkey leg tendon. Calcif Tissue Int 58:17–23
24. Paschalis EP, Jacenko O, Olsen B, Mendelsohn R, Boskey AL (1996) Fourier transform infrared microspectroscopic analysis identifies alterations in mineral properties in bones from mice transgenic for type X collagen. Bone 19:152–156
25. Walters MA, Leung YC, Blumenthal NC, Le Gros RZ, Konsker KA (1990) A Raman and infrared spectroscopic investigation of biological hydroxyapatite. J Inorg Biochem 39:193–200
26. Termine JD, Eanes ED, Greenfield DJ, Nylen MU, Harper RA (1973) Hydrazine-deproteinated bone mineral, physical and chemical properties. Calcif Tissue Res 12:73–90
27. Rey C (1984) Etude des relations entre apatites et composés moléculaires. Thèse d'Etat. Institut National Polytechnique de Toulouse
28. Tsuda H, Arends J (1994) Orientational Micro-Raman spectroscopy on hydroxyapatite single crystals and human enamel crystallites. J Dent Res 11:1703–1710
29. Penel G, Leroy G, Brès E (1998) A new preparation method of bone samples for Raman micro-spectrometry. Appl Spectroscopy 52:312–313
30. Penel G, Leroy G, Rey C, Sombret B, Huvenne JP, Brès E (1997) Infrared and Raman microspectrometry study of fluor-fluor-hydroxy and hydroxyapatite powders. J Mater Sci Mater Med 8:271–277
31. Puech PF, Dhamelincourt M, Taieb M, Serratrice C (1986) Laser Raman microanalysis of fossil tooth enamel. J Hum Evol 15:13–19
32. El Feky H, Rey C, Vignobles M (1991) Carbonate ions in apatites: infrared investigations in the ν_4 CO_3 domain. Calcif Tissue Int 49:269–274
33. Sfihi H, Legrand AP, Ranz X, Rey C (1996) Characterization of oxyhydroxyapatites by ^1H and ^{31}P solid-state nuclear magnetic resonance. Phos Res Bul (in press)
34. Fowler BO, Markovic M, Brown EW (1993) Octacalcium phosphate. 3. Infrared and Raman vibrational spectra. Chem Mater 5:1417–1423
35. Sauer GR, Wuthier RE (1988) Fourier Transform infrared characterization of mineral phases formed during induction of mineralization by collagenase-released matrix vesicles in vitro. J Biol Chem 263:13718–13724
36. Kim HM, Rey C, Glimcher MJ (1996) X-ray diffraction, electron microscopy, and Fourier transform infrared spectroscopy of apatite crystals isolated from chicken and bovine calcified cartilage. Calcif Tissue Int 59:8–63
37. Rehman I, Smith R, Hench LL , Bonfield W (1995) Structural evaluation of human and sheep bone and comparison with synthetic hydroxyapatite by FT-Raman spectroscopy. J Biomed Mater Res 29:1287–1294